Path Loss Characteristics Between Indoor Spaces in Different LOS Buildings

Masayuki Miyashita†, Hideki Omote†, Ryo Yamaguchi†
† R&D Division, SoftBank Corp.
Telecom Center Building East Tower 13F, 2-5-10 Aomi, Koto-ku, Tokyo, 135-0064 Japan
e-mail: † {masayuki.miyashita, hideki.omote, ryo.yamaguchi}@g.softbank.co.jp

***Abstract*—In order to overcome the increasing traffic problems of mobile terminals used in high-rise floors of buildings, the three-dimensional cell configuration which places small cells on various floors is considered. In order to evaluate the wireless transmission technology for the three-dimensional cell configuration, it is necessary to clarify the time-spatial characteristics which encompass the characteristics of the path loss, the delay profile and the spatial arrival angular profile for waves travelling from one indoor space in a high-rise office to another such indoor space. In this paper, we measure the path loss characteristics of radio waves passing from one indoor space to another and identify the key parameters for the path loss characteristic based on measured results. Further, we compare measured and simulation (ray tracing) results. Finally, we use the simulation results to analyze the relation between the parameters and path loss characteristics.**

Keywords—Data communication traffic, 3D cell structure, Ray trace, Path loss characteristics

I. INTRODUCTION

Recently, data traffic is explosively growing in cellular mobile communication systems due to the prevalence of smart phones and other terminals. In order to overcome the increasing traffic problems of mobile terminals used in high-rise buildings, the three-dimensional cell configuration which sets small cells on various floors is considered [1]-[5]. Fig.1 shows typical three-dimensional cell configurations [6]. In order to evaluate the wireless transmission technology used to implement the three-dimensional cell configuration, it is necessary to clarify the time-spatial characteristics for waves travelling from outdoor macro cells to indoor small cells as shown in (i) and (ii) of Fig.1, from indoor small cells to mobile phones on the road as shown in (iii) and (iv) of Fig.1 and from indoor small cells to other indoor small cells as shown in (v) and (vi) of Fig.1 [7]-[10]. Here, the time-spatial characteristics are composed of the characteristics of the path loss, the delay profile and the spatial arrival angular profile. In particular, the time-spatial characteristics of (v) and (vi) are strongly required given the increasing prevalence of high-rise small cells. We focus on the path loss characteristics of (v) and (vi), and note that while some research based on measured data has been reported [11]-[14], few studies have considered the detail mechanisms underlying the path loss characteristics of (v) and (vi).

In order to analyze the propagation mechanism of path loss characteristics in detail, it is necessary to extract key parameters based on measured results. In this paper, we measure the path loss characteristics for small cells in different buildings. We develop a ray trace system applicable to indoor-outdoor layouts in order to analyze each path characteristic. Finally, we analyze the relation between the parameters and path loss characteristics by using the ray tracing approach.

II. RADIO PROPAGATION MEASUREMENTS IN ACTUAL ENVIRONMENT

Figure 2 illustrates the measurement environment. We measured the path loss characteristics between two indoor spaces in different buildings in an urban area in Tokyo. The indoor spaces face each other. Both buildings are 100 m high, and their facing walls are separated by 45 m. Within each building, an approximately 30 m passage links a small room to the elevator hall. The indoor spaces on the same floors are in line of sight (LOS) to each other. We set the transmitting antenna in one building and the receiving antenna in the other building. We measure the path loss characteristics and analyze the dependency of vertical angle (θ).

A. Measurement condition

Table I summarizes measurement parameters. The carrier frequency is 3.35 GHz. We used sleeve antennas that are horizontal omni-directional at both sides. The transmitting antenna and the receiving antenna were both 1.5 m above their floors. The distance from window to transmitting antenna, d_1, was 4m. Window to receiving antenna distance, d_2, was 1 ~ 15 m. We measured received power while moving the receiving antenna. The measured values were converted into median values of penetration loss at 1 m increments.

The penetration loss is given by

$$\begin{aligned} Penetration\ loss = {} & P_{tx} + G_{tx\_ant} + G_{rx\_ant} - L_{cable} \\ & - L_{tx\_window} - L_{rx\_window} - P_{rx} - L_{freespace}. \end{aligned} \quad (1)$$

Note that P_{tx}, G_{tx_ant}, G_{rx_ant}, L_{cable}, L_{tx_window}, L_{rx_window}, P_{rx}, $L_{freespace}$ represent transmitting power, transmitting antenna gain, receiving antenna gain, cable loss, window transmission loss at transmitting side, window transmission loss at receiving side, received power, and propagation loss between the transmitting antenna and receiving antenna, respectively. For example, we calculate the measured penetration loss value at d_2 = 1 m. From Fig. 3, it is found that the value is approximately 14.56 dB for θ = 29 degrees.

Where the other values of Eq. (1) are 33.85 dB, 2.15 dB, 2.15 dB, 6.25 dB, 1.26 dB, 1.26 dB, −62.14 dB, 76.96 dB, respectively.

B. Measurement results

Figure 3 plots the measured penetration loss values for θ = 0 degrees and θ = 29 degrees. For θ = 0 degrees, it is found that the penetration loss characteristic remains unaffected by distance from the window. On the other hand, for θ = 29 degrees, the penetration loss increases with distance from the window. Therefore, both vertical angle and distance from the window influence the penetration loss characteristics.

III. Ray Trace

In order to analyze the mechanism underlying the propagation loss characteristics, it is necessary to clarify the impact of key parameters of each path arriving at the receiving antenna. In order to analyze each path characteristic, we developed a ray trace system applicable to indoor-outdoor layouts. We evaluate the accuracy of the system by using a simple indoor-outdoor layout simulating the measurement environment, see Figure 4. The layout sets two cuboids facing each other. Each is 2.5 m x 2.5 m x 30 m. The distance between the cuboids is 45 m, the same as the measurement environment. The vertical angle θ = 0 and 29 degrees.

A. Calculation condition

Table II summarizes parameters used in the calculation. The carrier frequency is 3.35 GHz. Both sides used horizontal omni-directional sleeve antennas. Both antenna heights were 1.5 m. The distance from window to transmitting antenna, d_1, was 4 m. We calculated the penetration loss at d_2 values from 1 to 15 m. The reflection and the diffraction numbers are 4 and 2 times, respectively.

B. Comparison of ray trace calculation and radio propagation measurement results

Figure 3 also plots the simulated penetration loss values for θ = 0 degrees and θ = 29 degrees. For θ = 0 degrees, it is found that the characteristic of penetration loss remains unaffected by distance from the window. On the other hand, for θ = 29 degrees, it is found that the penetration loss increases with the increasing distance from the window. This result basically matches the measured result, which confirms that the developed system could reproduce the characteristics of the measurement results.

IV. Analysis of Relation Between the Parameters and Propagation Loss Characteristics

We clarify the relation between the penetration loss characteristics and the key parameters.

Figure 5 shows path characteristics within 20 dB of maximum received power for θ = 0 degrees. The transmitting antenna was placed 4 m from the window. In Fig. 5 (a), the receiving antenna is 1 m from the window. In Fig. 5 (b), the receiving antenna is 13 m from the window. In both figures, the solid line plots the path yielding maximum received power. Therefore, the distance from the window has no impact on the penetration loss characteristics. The path of maximum received power is the LOS wave for θ = 0 degrees.

Figure 6 shows the same path characteristics for θ = 29 degrees, and d_1 = 4 m.

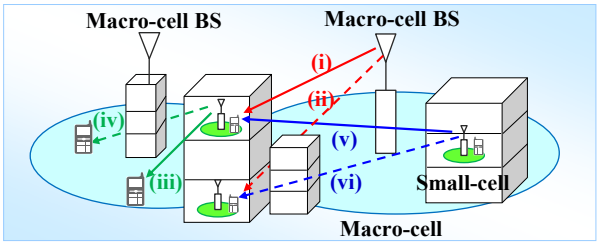

Figure 1. 3D cell structure

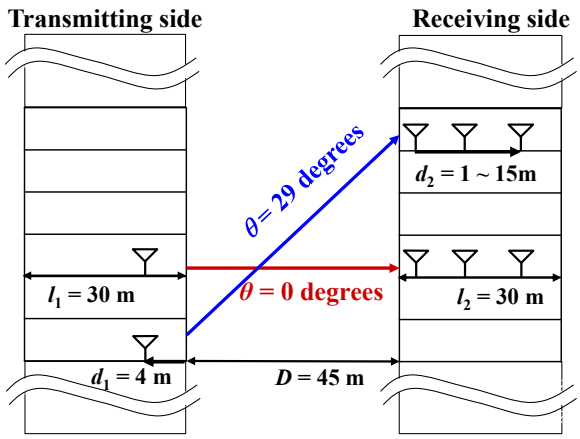

Figure 2. Measurement environment

Table I. Key measurement specifications

Frequency	3.35 GHz
Building height (Tx)	100 m
Building height (Rx)	100 m
Distance both buildings	45 m
Transmitting antenna	Sleeve antenna (horizontally non-directed)
Penetration distance (Tx antenna)	4 m
Antenna height (Tx)	1.5 m
Floor number (Tx)	11th, 13th
Receiving antenna	Sleeve antenna (horizontally non-directed)
Penetration distance (Rx antenna)	1 ~ 15 m
Antenna height (Rx)	1.5 m
Floor number (Rx)	13th, 16th
Ascending vertical angle	0, 29 degrees

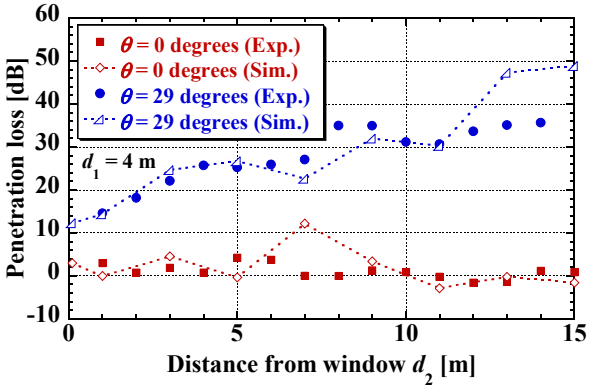

Figure 3. Characteristics of path loss

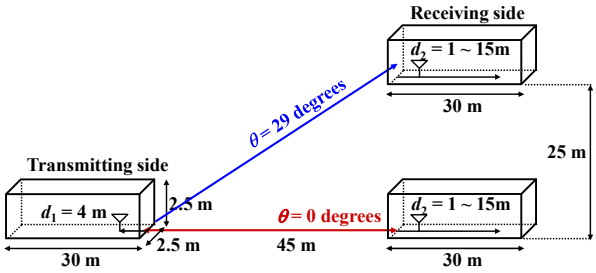

Figure 4. Indoor-outdoor layout

Table II. Key simulation specifications

Frequency	3.35 GHz
Distance both cuboids	45 m
Transmitting antenna	Sleeve antenna (horizontally non-directed)
Penetration distance (Tx antenna)	4 m
Antenna height (Tx)	1.5 m
Receiving antenna	Sleeve antenna (horizontally non-directed)
Penetration distance (Rx antenna)	1 ~ 15 m
Antenna height (Rx)	1.5 m
Ascending vertical angle	0, 29 degrees
Window opening	2.5 m x 2.5 m
Cuboid depth	30 m
Number of reflection	4 times
Number of diffraction	2 times

Fig. 6 (a) shows the result when d_2 = 1 m. The path of maximum received power includes one reflection on the transmitting side. Fig. 6 (b) shows the result when d_2 = 13 m. The path of maximum received power includes four reflections (i.e. one reflection on transmitting side and three reflections on receiving side). The results show that the penetration loss depends on d_2, when θ is large. Also, both

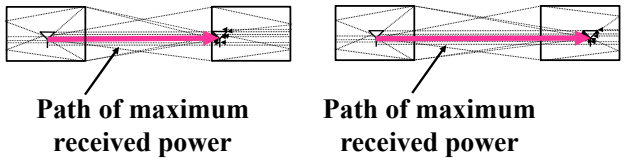

Figure 5. Path within 20 dB of maximum received power (d_1 = 4 m, θ = 0 degrees)

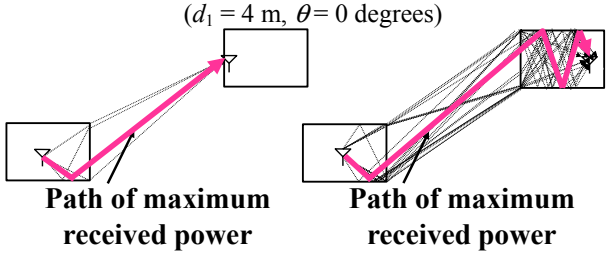

(a) d_1 = 4 m, d_2 = 1 m (b) d_1 = 4 m, d_2 = 13 m

Figure 6. Path within 20 dB of maximum received power (d_1 = 4 m, θ = 29 degrees)

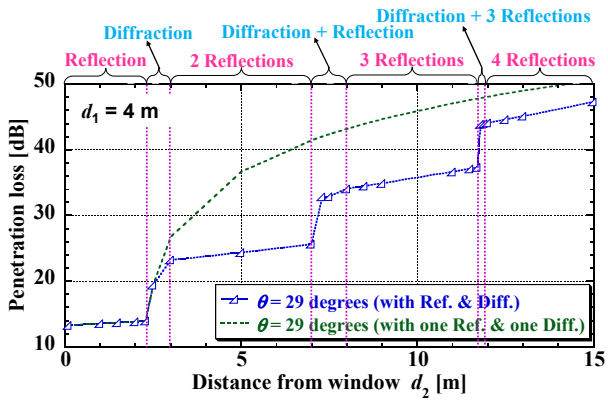

Figure 7. Penetration loss of maximum received power (θ = 29 degrees)

paths have one reflection on transmitting side, so the influence of both transmitting and receiving sides must be considered in estimating the path loss characteristics rooms that are not LOS.

Figure 7 shows the simulated penetration loss of maximum received power when d_1 = 4 m and θ = 29 degrees. For reference, this figure also shows the characteristics with one reflection on transmitting side and one diffraction event on receiving side. The path loss increases in a staircase pattern with the distance of receiving antenna from the window. It is because the change of propagation mechanism of the path. For example, the maximum path has one reflection in the range of d_2 = 0 ~ 2 m, but two reflections in the range of d_2 = 3 ~ 7 m.

V. Conculusion

We measured the path loss characteristics of radio waves from one high-rise office to another office in a different building and identified the key parameters for the path loss characteristics based on measured results. Further, we compared the measured results to the simulation results

yielded by our ray tracing based system. We confirmed that our system could reproduce the characteristics of the measured results. Finally, we analyzed simulation results and clarified the mechanism of propagation loss characteristics between offices.

ACKNOWLEDGMENT

This work was partially funded by the Ministry of Internal Affairs and Communications of Japan, under the grant, "R&D on 3-D dense cell structure and layered cell configuration technologies for mobile communication system".

We would also like to express our gratitude to Dr. Teruya Fujii for his support.

REFERENCES

[1] A. Damnjanovic, J. Montojo, W. Yongbin, J. Tingfang, T. Luo, M. Vajapeyam, T. Yoo, O. Song and D. Malladi, "A survey on 3GPP heterogeneous networks, " IEEE Wireless Commun., vol.18, no.3, pp.10–21, June 2011.

[2] 3GPP TR36.814 V9.0.0, "Further advancements for E-UTRA physical layer aspects," March 2010.

[3] 3GPP TR36.932 V12.1.0, "Study on scenarios and requirements of LTE small cell enhancements (Release 12)," March 2013.

[4] 3GPP TR36.872 V12.0.0, "Study on small cell enhancements for E-UTRA and E-UTRAN - Physical layer aspects (Release 12)," Sept. 2013.

[5] S. Konishi, "Comprehensive analysis of heterogeneous networks with pico cells in LTE-Advanced," IEICE Trans. Commun., vol.E96-B, no.6, pp.1243–1255, June 2013.

[6] A. Nagate, M. Mikami, T. Okamawari, T. Fujii, "A Proposal of Network-Based Coordinated Interference Reduction Technologies in 3D Cell Structure with eICIC," 2014 IEICE General Conf., B5–82, p.477, Mar. 2014.

[7] J. E. Berg, "4.6 building penetration," in "Digital Mobile Ratio Toward Future Generation System," COST Telecom Secretariat. Commision of the European Communities, Brussels, Belgium, pp.167–174, COST 231 Final Rep., 1999. sec. 4.6.

[8] H. Okamoto, K. Kitao, and S. Ichitsubo, "Outdoor–to–Indoor Propagation Loss Prediction in 800–MHz to 8–GHz Band for Urban Areas," IEEE Transaction on Vehicular Technology, Vol. 58, Issue 3, pp.1059–1067, Mar. 2009.

[9] T. Taga, "Prediction for Characteristics of Direction of Arrival in UHF-TV band Indoor Propagation Environment (I) : study on Geometrical Optics Calculation Method for Incident Radio Waves pass through Window Openings," IEICE Technical Report, A·P2006–38, pp.25–30, Jun. 2006.

[10] S. Komatsubara, K. Nishimori, K. Kitao, T. Imai, "Performance evaluation on interference temperature using measured outdoor, indoor and outdoor-indoor propagation data in heterogeneous networks," IEICE Technical Report, A·P2011–168, pp.125–130, Jan. 2012.

[11] I. Nagadome, Y. Miyata, S. Ichitsubo, H. Omote, T. Fujii, "Path loss Between Indoors of Different LOS Buildings for construction of 3D cells," IEICE Technical Report, A·P2013–199, pp.81–86, Mar. 2014.

[12] I. Nagadome, Y. Miyata, S. Ichitsubo, H. Omote, T. Fujii, "Path loss Between Indoors of Different Buildings in Micro-cell," 2014 IEICE General Conf., B1–35, p.28, Mar. 2014.

[13] T. Kuribayashi, R. Eguchi, S. Ichitsubo, H. Omote, T. Fujii, "Emission Pattern of the Indoor Base Station to Estimate the Indoor-Inddoor Propagation Loss," 2014 IEICE Society Conf., B1–27, p.27, Sept. 2014.

[14] W. Yamada, O. Holland, S. Ping, H. Aghvami, T. Sugiyama, "Building Entry Loss for Estimation of Interference Power between Buildings," 2014 IEICE General Conf., B1–29, p.29, Mar. 2014.